Progress In Electromagnetics Research Letters, Vol. 31, 199–207, 2012

MINIATURIZED MICROSTRIP DUAL-MODE FILTER WITH THREE TRANSMISSION ZEROS

S. Gao*, S. Xiao, and J.-L. Li

University of Electronic Science and Technology of China, Chengdu 610054, China

Abstract—A novel miniaturized microstrip dual-mode filter using a half wavelength resonator with centrally loaded open stub and quasi-L shaped feed-lines is proposed. The advantage of using such a resonator is inherently generating a transmission zero by itself. To further improve the selectivity, quasi-L shaped feed-lines are introduced to create additional transmission zeros. Theoretical and simulated analyses of this filter are performed. A demonstration filter centered at 2.33 GHz with a fractional bandwidth of 4.7% is designed, fabricated and measured to validate the design methodology.

1. INTRODUCTION

High performance microwave/RF bandpass filters are essential components in modern wireless communication systems. Among various filter topologies, dual-mode filters have attractive features such as high selectivity, compact size, and simple design. A dual-mode resonator can be considered as a doubly tuned circuit [1–11]. Thereby, the number of resonators for a given degree of filter is reduced, leading to a size reduction. In recent years, dual-mode resonators based on the even- and odd-mode operations have been extensively used in filter designs [12]. The Advantage of such a kind of resonator includes inherently generating a transmission zero by the resonator itself. To further improve the filter selectivity, source-load coupling was introduced to create additional transmission zeros [13, 14].

In this paper, a novel compact dual-mode bandpass filter with three transmission zeros is developed. The proposed filter is composed of a half wavelength resonator with centrally loaded open stub.

Received 30 March 2012, Accepted 28 April 2012, Scheduled 3 May 2012

* Corresponding author: Shanshan Gao (gaoshan5596@sina.com).

Meanwhile, quasi-L shaped feed-lines are introduced to create source-load coupling, thus generating extra transmission zeros near the passband. The even- and odd-mode methods are utilized to analyze the filter. Both theoretical and simulation studies are presented. A demonstration filter centered at 2.33 GHz is optimally designed, built and experimentally examined.

2. CIRCUIT DESIGN

Figure 1(a) illustrates the layout of the dual-mode resonator, composed of a half wavelength resonator with a loaded stub on its center plane. Even- and odd-mode methods can be adopted to analyze the resonator due to its symmetry. The odd-mode equivalent circuit is obtained by applying an electric wall (E wall) along the symmetry plane, as shown in Figure 1(b), resulting in short circuit in the odd-mode circuit. The input admittance is

$$Y_{ino} = 1/jZ_1 \tan\theta_1 \tag{1}$$

where Z_1 and $2\theta_1$ are the characteristic impedance and electrical length of the half wavelength line, respectively. At the resonance, the input admittance is zero. The first odd-mode resonance corresponds to

$$\theta_1 = \pi/2 \tag{2}$$

Similarly, the even-mode circuit is obtained by applying a magnetic wall (M wall) along the symmetry plane as illustrated in Figure 1(c), where open circuit formulates the case. From the figure we can see that the half wavelength resonator is loaded by an open stub along the M-wall. Thus, the even-mode resonance frequency can be easily adjusted to close to the first odd-mode resonance frequency due to the loaded

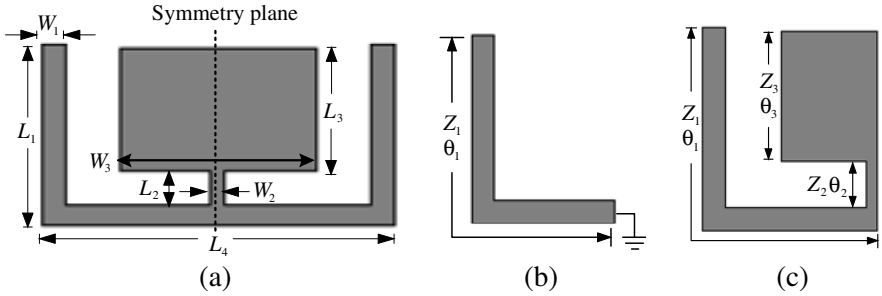

Figure 1. (a) Configuration of the dual-mode resonator. (b) Odd-mode circuit. (c) Even-mode circuit.

stub, resulting in even- and odd-mode-based dual-mode operations. The input admittance under even-mode operation is given by

$$Y_{ine} = \frac{\left[\begin{array}{l} 2Z_1Z_2\tan\theta_3 + 2Z_1Z_3\tan\theta_2 + 4Z_2Z_3\tan\theta_1 \\ -4Z_2^2\tan\theta_1\tan\theta_2\tan\theta_3 \end{array}\right]}{\left[\begin{array}{l} j(-4Z_1Z_2Z_3 + 4Z_1Z_2^2\tan\theta_2\tan\theta_3 \\ +2Z_1^2Z_2\tan\theta_1\tan\theta_3 + 2Z_1^2Z_3\tan\theta_1\tan\theta_2) \end{array}\right]} \tag{3}$$

where Z_2, θ_2, Z_3, and θ_3 are the characteristic impedances and electrical lengths of the two-section stepped stub, respectively. For the even-mode resonance, the resonance condition based on (3) is represented as

$$\begin{array}{l} 2Z_1Z_2\tan\theta_3 + 2Z_1Z_3\tan\theta_2 + 4Z_2Z_3\tan\theta_1 \\ -4Z_2^2\tan\theta_1\tan\theta_2\tan\theta_3 = 0 \end{array} \tag{4}$$

A full wave electromagnetic software (IE3D) was used to simulate the even- and odd-mode resonance frequencies under weakly coupled excitations. For all simulations, the substrate is of a relative permittivity of 9.6 and a thickness of 0.8 mm. The results are plotted in Figure 2 against the width W_3. It can be seen that when W_3 increases from 3.3 to 7.5 mm, the even-mode resonance frequency decreases almost linearly from 2.77 to 2.32 GHz. But the odd-mode resonance frequency is almost constant. The studied dual-mode resonator has an inherently finite transmission zero when the two modes split [12], as illustrated in Figure 2. When $f_e > f_o$, the transmission zero appears at the upper stopband, namely, $f_z > f_e$. Conversely, the zero is at the lower stopband when $f_e < f_o$. Thus, one finite transmission zero near

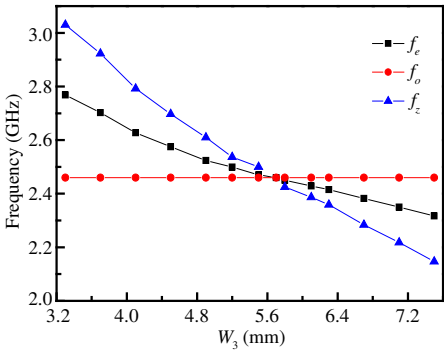

Figure 2. Simulated resonance frequencies of the even-mode, odd-mode and transmission zero with varying W_3 ($W_1 = 0.8$ mm, $W_2 = 0.5$ mm, $L_1 = 7$ mm, $L_2 = 1.3$ mm, $L_3 = 4.8$ mm, $L_4 = 12$ mm).

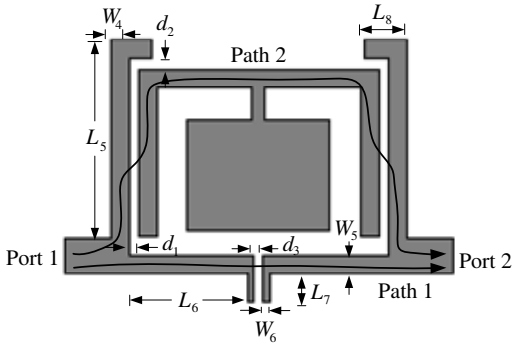

Figure 3. Layout of the proposed dual-mode filter.

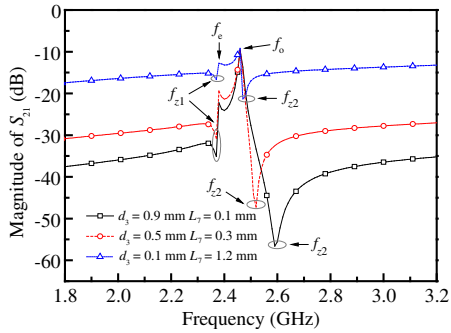

Figure 4. Simulated scattering parameters of the filter with path 1 only ($W_1 = 0.8\,\text{mm}$, $W_2 = 0.5\,\text{mm}$, $W_3 = 6.7\,\text{mm}$, $W_4 = 0$, $W_5 = 0.6\,\text{mm}$, $W_6 = 0.15\,\text{mm}$, $L_1 = 7\,\text{mm}$, $L_2 = 1.3\,\text{mm}$, $L_3 = 4.8\,\text{mm}$, $L_4 = 12\,\text{mm}$, $L_5 = 0$, $L_8 = 0$, $d_1 = 0.1\,\text{mm}$).

the passband can be easily obtained by adjusting the size of the loaded stub.

The developed filter topology is shown in Figure 3, where the feed-lines are a pair of quasi-L shaped lines. With this configuration, the source-load coupling is introduced. Now, two signal paths are passing through the filter. First, we only consider the path 1, thus the two vertical feed-lines are omitted. The simulated results are plotted in Figure 4. It is seen that there are two transmission zeros near the passband. Based on the above analysis, the lower transmission zero, f_{z1}, is generated from the dual-mode resonator itself for the case $f_e < f_o$.

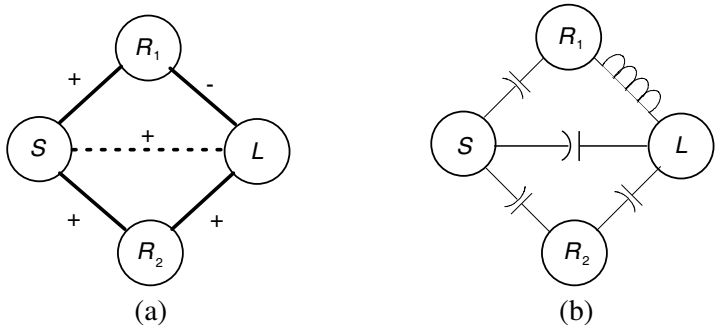

Figure 5. (a) Coupling scheme of the investigated dual-mode filter. (b) Coupling model when involving the coupling nature of the dual-mode filter.

To further analyze the transmission zeros, the coupling scheme of this filter is studied, as presented in Figure 5(a). The circles marked S and L denote source and load, or input and output, while R_1 and R_2 formulate the even-mode and odd-mode resonators. The input is coupled to both modes by the admittance inverters, represented by solid lines, and so is the output. Meanwhile, there is no coupling between the two modes. Moreover, the input and output are weakly coupled that is denoted by the dash line as described in Figure 5(a). In this coupling scheme, the main coupling is the input-$R_1(R_2)$-output; the direct coupling between the input and output is the secondary coupling. Based on the coupling scheme and the filter layout, it is derived that the coupling path, S-R_1-L, is capacitive-inductive, whereas another path, S-R_2-L, is capacitive-capacitive. The secondary coupling, S-L, is capacitive. Therefore, the introduced coupling scheme shown in Figure 5(a) can be further evolved to the one by involving the coupling nature, as illustrated in Figure 5(b). Now, the coupling model given in Figure 5(b) can be utilized to analyze the location of transmission zeros. Notice that the phase components (Φ_{21} and Φ_{11}) of the S-parameters S_{21} and S_{11} for a two-port network can be expressed by

$$\Phi_{21} \approx -90^\circ \text{ (for shunt inductor and capacitor resonators above resonant frequency)} \quad (5a)$$

$$\Phi_{21} \approx +90^\circ \text{ (for shunt inductor and capacitor resonators below resonant frequency)} \quad (5b)$$

$$\Phi_{21} \approx -90^\circ \text{ (for series inductors)} \quad (5c)$$

$$\Phi_{21} \approx +90^\circ \text{ (for series capacitors)} \quad (5d)$$

Table 1. Total phase shifts between input and output based on Figure 5(b).

	Below Resonant Frequency	Above Resonant Frequency
Path S-R_1-L	$+90^\circ + 90^\circ - 90^\circ = +90^\circ$	$+90^\circ - 90^\circ - 90^\circ = -90^\circ$
Path S-R_2-L	$+90^\circ + 90^\circ + 90^\circ = +270^\circ$	$+90^\circ - 90^\circ + 90^\circ = +90^\circ$
Results	Out of phase	Out of phase

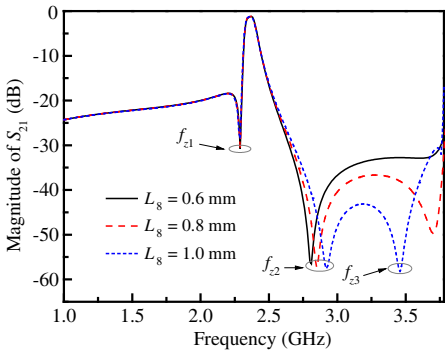

Figure 6. Simulated scattering parameters of the filter for varying L_8 ($W_4 = 0.6\,\text{mm}$, $W_5 = 0.6\,\text{mm}$, $W_6 = 0.15\,\text{mm}$, $L_5 = 7.64\,\text{mm}$, $L_6 = 5.9\,\text{mm}$, $L_7 = 1.0\,\text{mm}$, $d_1 = 0.1\,\text{mm}$, $d_2 = 0.1\,\text{mm}$, $d_3 = 0.1\,\text{mm}$).

Using these relationships, the phase shifts can be found for possible signal paths. When summing the phase-shift contributions of the individual components, resonators R_1 and R_2 must be considered both below and above the resonant frequencies. Table 1 summarizes the total phase shifts between input and output based on Figure 5(b). It is interesting to note that signal passing through several possible paths has out of phase, which means transmission zeros close to lower and upper passbands of the filter can be generated. Therefore, this analytically explains the zeros, f_{z1} and f_{z2}, in Figure 4.

To further improve the selectivity, path 2 is introduced as illustrated in Figure 3. The locations of the third transmission zero can be controlled by tuning the length of the loaded stub, i.e., L_8. Figure 6 illustrates the simulated scattering parameters of the dual-mode filter with varying the parameter L_8. As shown in Figure 6, the third transmission zero, f_{z3}, is generated. The position of f_{z3} moves towards the lower frequency when L_8 increases from 0.6 to 1.0 mm. In addition, there is little influence on the locations of f_{z1} and f_{z2}. On

the other hand, the use of vertical feed-lines also enhances the coupling between the resonator and the feed-lines, thus minimizing the insertion loss within the passband.

3. SIMULATED AND MEASURED RESULTS

The designed filter was fabricated and measured. Measurement was carried out on Agilent E8363B network analyzer. Figure 7 shows the simulated and measured results of the proposed dual-mode filter. From the measured results, it is seen that the dual-mode filter operates at the center frequency of 2.33 GHz with fractional bandwidth of 4.7%. The insertion loss within the passband is approximately 2 dB. Three transmission zeros located at 2.24, 3.04 and 3.47 GHz with attenuations over 22.8, 59.6 and 59.7 dB are respectively implemented.

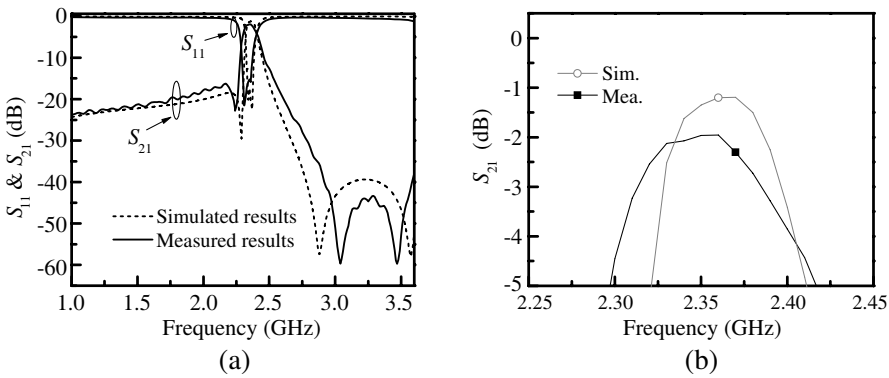

Figure 7. (a) Simulated and measured broadband frequency responses of the proposed dual-mode filter. (b) Simulated and measured narrow band frequency responses of the proposed dual-mode filter.

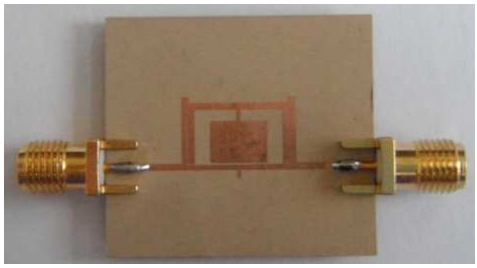

Figure 8. Photograph of the fabricated dual-mode filter.

The center frequency from simulation is 2.36 GHz against 2.33 GHz from measurements, which has an error approximately 1.3%. This tolerance is acceptable in most engineering applications. The circuit size is about $13.4 \times 9.4\,\text{mm}^2$, corresponding to $0.32\lambda_g \times 0.23\lambda_g$ when referred to the guided-wavelength at the center frequency. Figure 8 shows the photograph of the proposed dual-mode filter.

4. CONCLUSION

A compact microstrip dual-mode filter based on even- and odd-mode operations has been studied. The transmission zeros generated by the developed filter have been theoretically and simulatively investigated. A demonstration filter has been designed and experimentally confirmed to validate the design concept. The developed filter topology features compactness, easy fabrication and is suitable for high performance microwave systems.

ACKNOWLEDGMENT

This work was in part supported by the Fundamental Research Funds for Central Universities under contract No. E022050205 and in part by the National Natural Science Foundation of China under contract Nos. 60872034 and 60971029.

REFERENCES

1. Luo, S., L. Zhu, and S. Sun, "A dual-mode dual-band bandpass filter using a single slot ring resonator," *Progress In Electromagnetics Research Letters*, Vol. 23, 173–180, 2011.
2. Zhang, L., Z.-Y. Yu, and L. Guo, "Compact planar triple-mode bandpass filter with enhanced parasitic coupling," *Journal of Electromagnetic Waves and Applications*, Vol. 24, No. 4, 495–503, 2010.
3. Tyurnev, V. V. and A. M. Serzhantov, "Dual-mode split microstrip resonator for compact narrowband bandpass filters," *Progress In Electromagnetics Research C*, Vol. 23, 151–160, 2011.
4. Esfeh, B. K., A. Ismail, R. S. A. Raja Abdullah, H. Adam, and A. R. H. Alhawari, "Compact narrowband bandpass filter using dual-mode octagonal meandered loop resonator for WiMAX application," *Progress In Electromagnetics Research B*, Vol. 16, 277–290, 2009.

5. Wang, Y. X., B.-Z. Wang, and J. P. Wang, "A compact square loop dual-mode bandpass filters with wide stop-band," *Progress In Electromagnetics Research*, Vol. 77, 67–73, 2007.
6. Wolff, I., "Microstrip bandpass filter using degenerate modes of a microstrip ring resonator," *Electron. Lett.*, Vol. 8, No. 12, 302–303, Jun. 1972.
7. Hong, J.-S. and M. J. Lancaster, "Microstrip bandpass filter using degenerate modes of a novel meander loop resonator," *IEEE Microw. Guided Wave Lett.*, Vol. 5, No. 11, 371–372, Nov. 1995.
8. Zhu, L., P.-M. Wecowski, and K. Wu, "New planar dual-mode filter using cross-slotted patch resonator for simultaneous size and loss reduction," *IEEE Trans. Microw. Theory Tech.*, Vol. 47, No. 5, 650–654, May 1999.
9. Zhu, L., C. T. Boon, and S. J. Quek, "Miniaturized dual-mode bandpass filter using inductively loaded cross-slotted patch resonator," *IEEE Microw. Wireless Compon. Lett.*, Vol. 15, No. 1, 22–24, Jan. 2005.
10. Mao, R.-J. and X.-H. Tang, "Novel dual-mode bandpass filters using hexagonal loop resonators," *IEEE Trans. Microw. Theory Tech.*, Vol. 54, No. 9, 3526–3533, Sep. 2006.
11. Mao, R.-J., X.-H. Tang, and F. Xiao, "Miniaturized dual-mode ring bandpass filters with patterned ground plane," *IEEE Trans. Microw. Theory Tech.*, Vol. 55, No. 7, 1539–1547, Jul. 2007.
12. Hong, J.-S., H. Shaman, and Y.-H. Chun, "Dual-mode microstrip open-loop resonators and filters," *IEEE Trans. Microw. Theory Tech.*, Vol. 55, No. 8, 1764–1770, Aug. 2007.
13. Zhang, X.-C., Z.-Y. Yu, and J. Xu, "Design of microstrip dual-mode filters based on source-load coupling," *IEEE Microw. Wireless Compon. Lett.*, Vol. 18, No. 10, 677–679, Oct. 2008.
14. Li, L. and Z.-F. Li, "Application of inductive source-load coupling in microstrip dual-mode filter design," *Electron. Lett.*, Vol. 46, No. 2, 141–142, Jan. 2010.